Phonon-emission spectroscopy of a two-dimensional electron gas

M. Rothenfusser, L. Köster, and W. Dietsche
Physik-Department (E-10), Technische Universität München, D-8046 Garching bei München, West Germany
(Received 24 April 1986)

A two-dimensional electron gas (2D EG) was created in a metal-oxide-semiconductor structure on a (100) surface of Si at a temperature of 1 K. Transport of electric current through the 2D EG led to power dissipation and the emission of acoustical phonons. We used superconducting tunnel junctions as phonon detectors and found that the phonon-frequency spectrum had a $2k_F$ cutoff. As a consequence of the reduced dimensionality of the electrons the cutoff frequency depended also on the phonon-emission angle. The phonon intensity emitted under oblique angles was asymmetric and depended on the current direction (phonon-drag effect). These properties are in contrast to what one would expect from a 3D blackbody source. We calculated the expected spectra using the energy and momentum conservation laws applied to the interaction between 2D electrons and 3D phonons and found good agreement with the experimental results as long as the electron densities did not exceed 4×10^{12} cm^{-2}. At larger densities additional features were observed which are not yet understood.

I. INTRODUCTION

It is well established that electron layers can form at semiconductor interfaces. These layers show very distinct two-dimensional (2D) properties,[1] but they nevertheless interact with their three-dimensional (3D) surroundings by, e.g., the emission and absorption of phonons. This interaction between excitations of different dimensionalities could show interesting effects, particularly because the respective values of the energies and wave vectors of the phonons are comparable to those of the electrons. However, very little experimental work about this interaction has been published so far.

The absorption of ballistic heat pulses by 2D electrons was observed by Hensel *et al.*[2] It was found that the absorptivity had the correct order of magnitude after phonon interference effects were taken into account. Particularities due to the lower dimensionality of the electron gas, however, could not be seen clearly because of limited spectral resolution.

Phonons emitted from 2D electrons in GaAs heterolayers were observed by Chin *et al.*[3] The results differed from those obtained with 3D electrons. But spectral resolution was again limited and no detailed analysis was made.

In other experiments, the temperature and the energy-loss rates under hot-electron conditions were determined.[4,5] These quantities describe very integral properties, however, and do not yield much information about the underlying quantum processes.

In this article, we report on experiments with a spectral analysis of the phonons emitted by a two-dimensional electron gas (2D EG). The phonons were detected with both broadband and narrow-band phonon detectors. In the data, we found a replica of the electron-distribution function. A very striking dependence of the phonon spectra on emission angle could be traced back to the partial lifting of the wave-vector—conservation laws at the surface. Furthermore, a phonon-drag effect could be observed if the electron gas was drifting.

In the following two sections of this article we will describe the experimental techniques and the results of the phonon experiments, respectively. Theoretical calculations of the phonon spectra will be presented in Sec. IV. A comparison of the theory with the data will be made in Sec. V.

II. EXPERIMENTAL TECHNIQUES

The 2 D EG, studied in this work, was formed in standard metal-oxide-semiconductor (MOS) structures. The design is shown schematically in Fig. 1. Squares (15×15 mm^2) of 3 mm thickness were cut from n-type doped (300 Ω cm) Si.[6] The surfaces were (100)-oriented. One sample side was oxidized forming a SiO_2 layer about 150 nm thick.[7] A Ni-Cr film 10 nm thick was deposited on top of

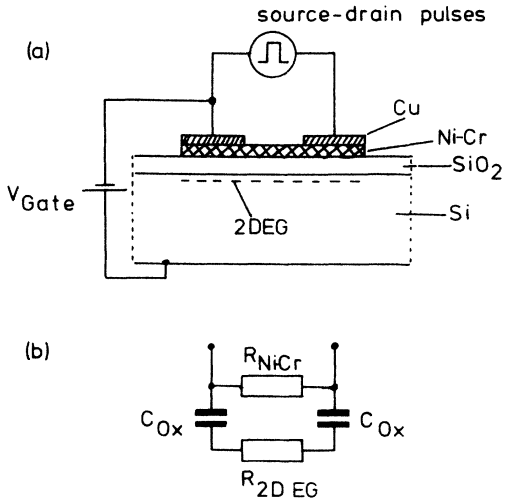

FIG. 1. (a) Sample setup (not to scale). The electron gas forms at the Si-SiO_2 interface if a voltage is applied to the NiCr gate. (b) Schematic of the source-drain circuit. The impedance of C_{ox} can be neglected for 100 ns pulses. Thus R_{NiCr} and the 2D EG can be treated as parallel resistances.

the oxide serving as the gate electrode. The 2 D EG formed as an accumulation layer if a voltage V_0 was applied to the gate with respect to the substrate.[8] The carrier density N_s in the 2 D EG is given by the relation $N_s=(C_{ox}/e)(V_0-V_t)$, where V_t is the threshold voltage and C_{ox} is the capacitance of the oxide per unit area.

The source-drain contacts were made capacitively with two 100-nm-thick Al films covering the ends of the NiCr film.[9] An active channel area between the contacts was left as a square with an area of 1 mm^2. In Fig. 1(b) the diagram of the source-drain circuit is shown.

The source-drain voltage V_{SD} was applied as pulses of 100 ns duration. Thus the impedance of the capacitances $C_{OX}\approx 1$ nF was small compared with the typical resistance values of the electron channel $R_{2DEG}\approx 1$ kΩ and the NiCr film $R_{NiCr}\approx 10$ kΩ. The peak electron mobilities in our samples varied from 3000 to 5000 cm^2/V sec.

If a source-drain field E_{SD} is applied along a 2D EG, then an electric current $j=N_s e\mu E_{SD}$ is caused and the electric power will eventually be transferred into phonon modes of the Si substrate. The power density was typically 1 mW/mm^2 in our experiments. In a three-dimensional heater film this power density would raise its temperature from an ambient 1 K to about 2 K. The phonon spectrum would be that of a blackbody with a dominant phonon frequency of about 150 GHz.[10] In that frequency regime phonons travel ballistically through the Si substrate.[11]

As phonon detectors we used superconducting tunnel junctions.[12] Such devices consist of two superconducting films about 150 nm thick, separated by a thin oxide layer. The operation of the junctions required an ambient temperature of 1 K. The tunnel current depends on the phonon flux absorbed in the junction if it is biased below the gap voltage $2\Delta/e$. Phonons, however, will be absorbed in the superconducting films only if their frequencies exceed the respective energy gap $2\Delta/h$. Thus one has a detection threshold which is 650 GHz for Pb and 100 GHz for Al as superconductors.

The experimental setup is sketched as an inset in Fig. 2. The detectors monitored the phonon flux traversing the Si sample under the geometrical angle ϑ. Due to phonon-focusing effects in the bulk Si, the wave-vector directions of these phonons were, in general, not colinear with the propagation directions.[13] The angle θ between the wave vector and the surface normal was calculated from ϑ using standard elastic theory. Later we will always refer to the wave-vector angle θ.

At very high frequencies the propagation of phonons is limited by the elastic scattering caused by the different Si-isotope masses.[14] This effect reduced the intensities of the phonon pulses by the factor $\exp(-Alf^4/v_s)$, where A is a material constant of Si, l is the phonon-path length, f is the phonon frequency, and v_s is the sound velocity.

The isotope scattering becomes effective at frequencies exceeding 800 GHz. If scattered phonons still reach the detector then they have longer path lengths and can therefore be separated from the unscattered ones by their longer times of flight. Combined with the sensitivity threshold of the tunnel-junction detectors, the isotope scattering has the effect of forming a sensitivity window. It is rather narrow (650—800 GHz) for Pb and very broad (100—800 GHz) for Al, respectively. This window property had been exploited before.[15] A theoretical analysis has also been published.[16]

III. EXPERIMENTAL RESULTS

An example of a phonon signal as a function of time of flight is shown in Fig. 2 (Al detector). At $t=$ zero, a source-drain pulse was applied to the MOS structure causing some electronic crosstalk. At later times, longitudinally (LA) and transversely (TA) polarized phonons were detected after their respective times of flight.

In the course of an experiment we measured first the source-drain current pulse. From it the conductivity $\sigma_\square$ and the dissipated power ($E_{SD}=$const) was deduced. Second, the intensities of the phonon pulses at their leading edges were recorded. Both the dissipated power and the phonon signal were measured as a function of gate voltage or, equivalently, carrier concentration N_s.

In Fig. 3 the conductivity data of a sample with an electron peak mobility of 4800 cm^2/V sec are shown. The behavior was as expected.[1] The concurrent TA-phonon signal as measured with an Al detector is shown in Fig. 4 (solid line). Not surprisingly, the course of the phonon signal followed roughly the dissipated power because a broadband detector was used. Similar traces were obtained for other angles too.

In the next experiment, we used the narrow-band Pb detector. Results for TA and LA phonons are shown in Figs. 5 and 6, respectively (solid lines). Only data pertaining to the electrons are presented since no signal was observed with holes as carriers. Apparently, the phonon spectrum emitted by the holes lies completely below the detection threshold of the Pb detector.

The three sections of Fig. 5 correspond to different angles between the phonon wave vector and the surface normals. In all three cases the phonon signal no longer fol-

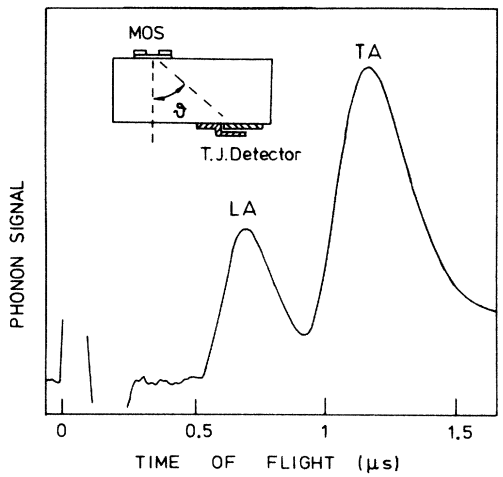

FIG. 2. Phonon signal as a function of time of flight. The two phonon pulses with different polarization are clearly separated. Inset: geometry of MOS phonon generator and tunnel-junction detector.

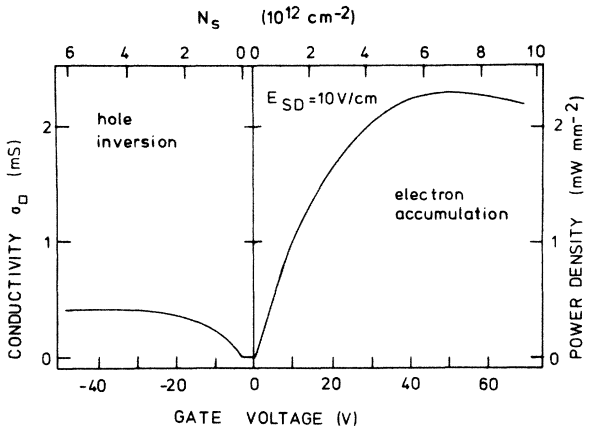

FIG. 3. Conductivity of a MOS sample as a function of gate voltage (or equivalently carrier density N_s). At negative gate voltages a 2D hole gas forms. The dissipated power with a source-drain field of 10 V/cm can be read from the scale at the right-hand side.

lowed the dissipated power. Even more striking, the traces were different from each other for different angles. A steep increase was observe which occurred, however, at the smaller N_s values for the smaller θ. At about $N_s=5\times10^{12}$ cm^{-2} there was a hump which was more pronounced for smaller θ. The signal decreased down to zero if N_s exceeded 6×10^{12} cm^{-2}. These two features were observed at all angles.

The LA phonons were measured at one angle, $\theta=63°$, only because at smaller angles they are "defocused" and too weak to be observed. This angle was rather large as compared with the TA-phonon results of Fig. 5. However, the signal increase occurred at very small densities already. The signal decrease, however, was observed at about the same N_s value as with the TA phonons. The hump at about $N_s=5\times10^{12}$ cm^{-2} was again visible.

The dependence of the phonon signal on emission angle and polarization is in contrast to the results which one would expect from a three-dimensional heater. It would emit a blackbody spectrum independent of angle and polarization.

The phonon results also depended on the magnitude and the polarity of E_{SD}. The data are shown in Fig. 7

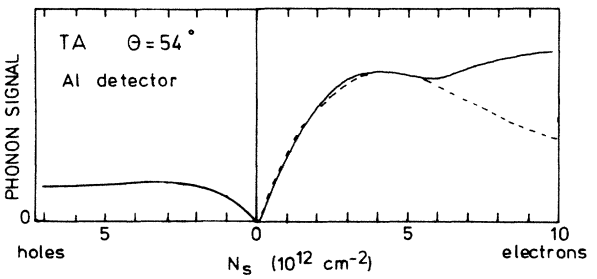

FIG. 4. Phonon emission of the sample of Fig. 3 measured with a broadband detector as a function of hole and electron density, respectively. Dashed line: theory.

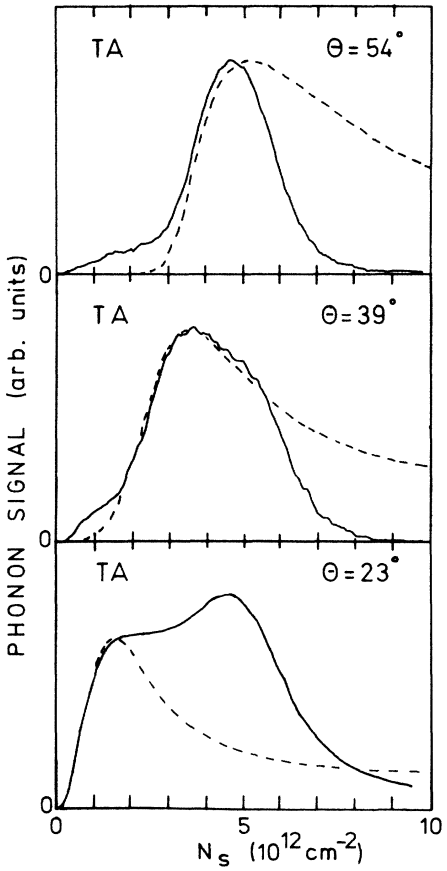

FIG. 5. Phonon emission of the same sample as in Figs. 3 and 4 but measured with the narrow-band Pb tunnel-junction detector. The three parts of the figure correspond to different angles between the phonon wave vectors and the surface normal. The angle-dependent signal increase is a consequence of the $2k_F$ cutoff being swept over the detector window. Dashed lines are theoretical results.

(solid lines). The three data sets correspond to the fields ±10, ±100, and ±200 V/cm, respectively. The general trend was that the sharp features found with small fields smear out with increasing fields. Strikingly, there was always a difference in signal size if the polarity of E_{SD} was

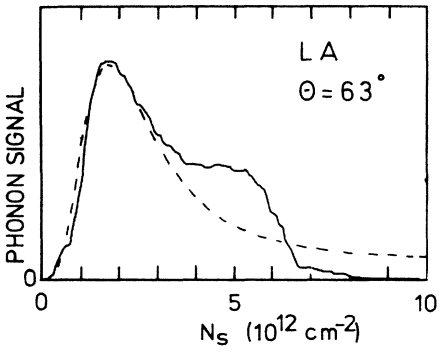

FIG. 6. Same as Fig. 5, but longitudinal instead of transverse polarization. The signal increase occurs already at a very small N_s value.

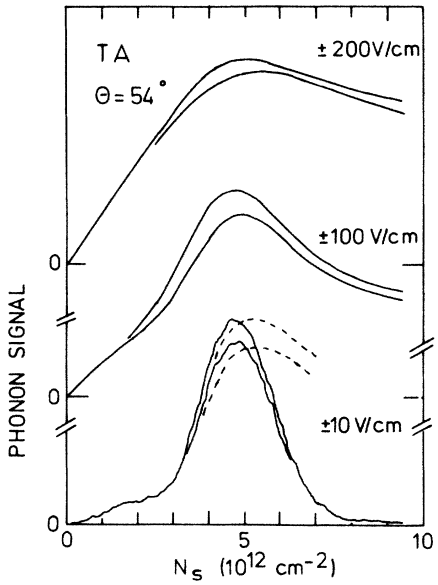

FIG. 7. The phonon signal measured at different source-drain fields with a Pb junction detector. At larger fields (higher electron temperatures) the features smear out. The difference in signal size with reversed field polarity is due to a phonon-drag effect.

reversed. The signal was larger if E_{SD} was pointing in such a way that the electrons drifted towards the detector.

In the next section we will show that many but not all of these results can be explained by a simple model of the phonon emission process in a 2D EG.

IV. THEORY

In bulk Si the surfaces of constant electron energy are six degenerate ellipsoids. In a 2D EG the degeneracy is partially lifted. The two bands, in which the effective mass perpendicular to the surface is larger, have the lower energy. If the surface normal is the z direction then the energy of the electrons in this band is given by

$$E=E_0+\frac{\hbar^2}{2m^*}(k_x^2+k_y^2)\ , \tag{1}$$

where m^* is the (light) effective mass and E_0 is the energy at the band bottom. The Fermi vector k_F depends on N_s according to

$$k_F=(2\pi N_s/g_v)^{1/2}\ , \tag{2}$$

where $g_v=2$ is the valley degeneracy.

The electron mobility in the 2D EG is determined by the momentum-relaxation rate. The most effective process for momentum relaxation at low temperatures is scattering at charged impurities in the oxide. It turns out that electron-phonon scattering is much less likely and, therefore, only determines the energy-loss rate.

The following calculations are based on the assumption that phonons are emitted during the transition of an electron from state $\mathbf{k}^i$ to state $\mathbf{k}^f$ within the lowest subband under emission of a bulk acoustical phonon with wave vector $\mathbf{q}$. The 2D EG is considered to be a sheet in an infinite medium. This appears to be an acceptable simplification because the acoustic mismatch between Si and SiO_2 is very small.[17,18] Optical phonons will be unimportant as long as $k_B T_{el} \ll \hbar\omega_{op} \approx 50$ meV (T_{el}: electron temperature; ω_{op}: optical phonon frequency). It is further assumed that the electron-energy distribution is described by k_F, drift velocity v_d, and T_{el}. Since T_{el} turned out to be considerably higher than the ambient temperature, stimulated processes could be neglected.

Energy-loss rates to the phonons have been calculated by several workers.[1,4,19] We, however, are interested in the exact shape of the phonon spectrum emitted into a certain direction. Therefore, a detailed calculation was made taking the anisotropies of the phonons and of the deformation potential into account precisely. Furthermore, screening was also included.

The emission rate of phonons with wave vector $\mathbf{q}$ is given by

$$\Gamma_q=2g_v\frac{2\pi}{\hbar}\sum_{\mathbf{k}}\frac{|\mathcal{M}|^2}{[\epsilon(q_p,\omega)]^2}f_d(E(\mathbf{k}^i))[1-f_d(E(\mathbf{k}^f))]$$
$$\times\delta(E(\mathbf{k}^i-E(\mathbf{k}^f)-\hbar\omega)\ , \tag{3}$$

where $\mathcal{M}$ is the matrix element of the electron transition, $\epsilon(q_p,\omega)$ describes the screening, and f_d is the Fermi distribution function in which the drift of the electrons by $m^* v_d/\hbar$ is included.

In Si the matrix element is determined by the deformation potential.[20] Thus, for the (100) plane

$$\mathcal{M}=\frac{1}{A}\int d\mathbf{r}\,\zeta(z)\exp(i\mathbf{k}^i\cdot\mathbf{r}_p)$$
$$\times[\Xi_d(\epsilon_{xx}+\epsilon_{yy}+\epsilon_{zz})+\Xi_u\epsilon_{zz}]\zeta(z)$$
$$\times\exp(-i\mathbf{k}^f\cdot\mathbf{r}_p)\ , \tag{4}$$

where $\Xi_u=9.0$ eV and $\Xi_d=-6.0$ eV are the two components of the deformation potential,

$$\epsilon_{ij}=\frac{1}{2}\left[\frac{\partial u_i}{\partial x_j}+\frac{\partial u_j}{\partial x_i}\right] \tag{5}$$

are the components of the strain tensor of the phonon $\mathbf{q}$,

$$\zeta_0(z)=(2a_0^3)^{-1/2}z\exp(-z/2a_0)$$

is the amplitude of the electron wave function, a_0 is a thickness parameter, and A is the area. The index p refers to components within the 2D EG plane. The displacement of the phonon with the polarization $\mathbf{p}$ is given by

$$\mathbf{u}(\mathbf{r})=\mathbf{p}\left[\frac{\hbar}{2\omega\rho V}\right]^{1/2}e^{-i\mathbf{q}\cdot\mathbf{r}}\ , \tag{6}$$

where $\rho=2.33$ g cm^{-3} and V are the density and the volume of the crystal, respectively. It follows from (4) that $\mathcal{M}\neq 0$ only if

$$\mathbf{k}^i-\mathbf{k}^f=\mathbf{q}_p\ . \tag{7}$$

The integration of (4) over z leads to a form factor

$$G(q_z)=\frac{1}{[1+(q_z a_0)^2]^3} . \tag{8}$$

The screening was calculated from the dynamic Lindhard theory

$$\epsilon(q_p,\omega)=1+\frac{2\pi\beta\chi(q_p,\omega)}{\kappa}F(q_p) , \tag{9}$$

with the parameters having the same meaning as in Ref. 1. The screening form factor $F(q_p)$ reduces the screening because of the finite thickness of the 2D EG.[21]

To evaluate the sum over the $\mathbf{k}$ states in (1) we choose the coordinates that $\mathbf{q}=(q_x,0,q_z)$. The argument of the δ function is zero at

$$k_x^i=\frac{q_p}{2}+\frac{m^*}{\hbar}v_s\frac{q}{q_p} . \tag{10}$$

This defines the $\mathbf{k}^i$ states which are allowed from energy and momentum conservation. Now (1) can be rewritten as

$$\Gamma_q=2g_v\frac{|\mathcal{M}|^2}{[\epsilon(q_p,\omega)]^2}\frac{Am^*}{2\pi\hbar^3 q_p}\times\int dk_y^i f_d(E(\mathbf{k}^i))[1-f_d(E(\mathbf{k}^f))] . \tag{11}$$

Inspection of (10) and (11) shows, firstly, that the maximum q_p is of the order of $2k_F$, a feature known as the $2k_F$ cutoff. Thus, since $q=q_p/\sin\theta$, the maximum q value must depend on the emission angle. Secondly, if the electron temperature T_{el} approaches zero then phonon emission is possible only if the x component of the drift velocity is equal to $v_s/\sin\theta$. The condition $T_{el}=$ zero can not be met in standard MOS devices because of the finite resistance due to impurity scattering. Thus, in order to make the electric power equal to the phonon emission, T_{el} must rise drastically, even at small fields. The resulting thermal smearing of the Fermi distribution leads to sufficient phase space for electron transitions.

The elastic constants used to evaluate (3) were taken from Ref. 17. The electron temperature T_{el} was obtained from a variational procedure. Summing of (11) over all phonon modes yielded the total emitted phonon power

$$\dot{Q}_{theor}=\sum_q \hbar\omega_q\Gamma_q . \tag{12}$$

The value of T_{el} was adjusted until $Q_{theor}=Ae\mu N_s E_{SD}^2$, the dissipated electrical power. The resulting T_{el} values are plotted as a function of N_s in Fig. 8 for the sample of Fig. 3 and an $E_{SD}=10$ V/cm. It turned out that the temperatures varies between 12 and 18 K.

These temperature values were used to calculate the phonon emission spectra. These were obtained by summing (12) only over the phonons which could hit the detector. The angle was set to be $\theta=54°$. In Fig. 9 (top) the LA-phonon intensity is plotted as a function of phonon energy. The three traces correspond to the Fermi vectors 1×10^6 cm^{-1}, 3×10^6 cm^{-1}, and 5×10^6 cm^{-1}, respectively. The common feature is the very pronounced peak with a cutoff towards higher frequencies. In the cutoff region the q_p component of the phonon wave vector is equal to $2k_F$. The TA phonons show a similar behavior

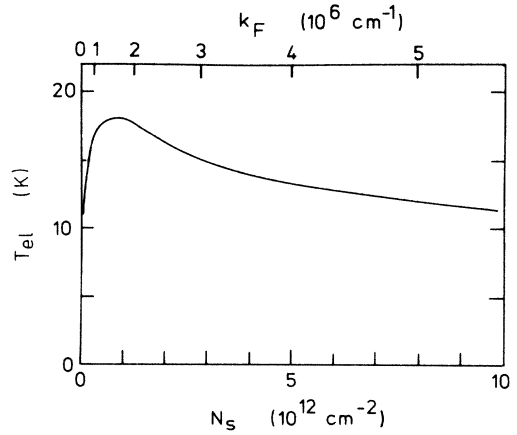

FIG. 8. Theoretical electron temperatures as a function of N_s. The corresponding k_F values are at the top. The parameters are those of Fig. 3.

[Fig. 9 (bottom)] except that the condition $q_p=2k_F$ is already fulfilled at smaller phonon energies.

Also shown in Fig. 9 is the effect of reversing the E_{SD} field direction. If carriers are drifting away from the detector, then the intensity is smaller (dotted lines). This phonon-drag effect is rather small in our samples because the thermal smearing is large compared with the drift of the carriers.

In Fig. 10 the emission angle θ is varied (TA phonons, $k_F=3\times10^6$ cm^{-1}). At small values the maximum

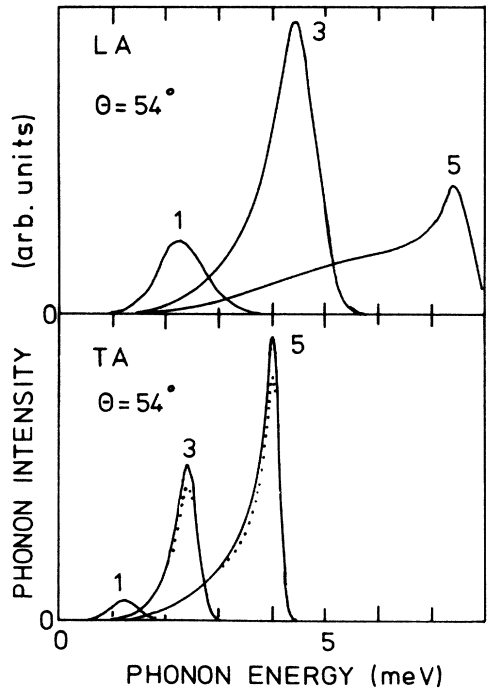

FIG. 9. Theoretical phonon spectra. The two parts correspond to LA and TA phonons. In each case the spectra are given for three k_F values in units of 10^6 cm^{-1}. In the case of the TA phonons the effect of reversing the drift-velocity direction is also shown (dotted lines).

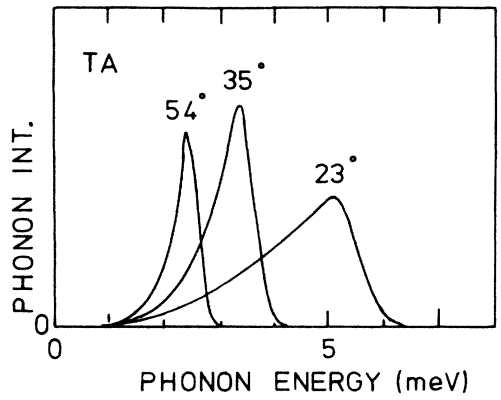

FIG. 10. Theoretical spectra with a $k_F = 3 \times 10^6$ cm^{-1} calculated for different angles θ.

$q \approx 2k_F/\sin\theta$ can become very large. A singularity in the phonon emission, however, is prevented by the finite T_{el} and the screening.

Thus to conclude the theoretical section, we have found that the two dimensionality of the carriers affects the emitted phonon spectra profoundly. These depend on the Fermi vector, the emission angle, the phonon polarization, and the E_{SD} field direction.

V. DISCUSSION

In the experiment, we used phonon detectors which were sensitive for a fixed frequency band. By variation of N_s the frequency spectrum was swept over this band.

Several qualitative conclusions can be drawn immediately from the theoretical spectra in Figs. 9 and 10. First, by increasing N_s, or equivalently k_F, the peak in the theoretical spectra moves to higher phonon energies. As soon as it coincides with the sensitivity band of the detector a steep signal increase is expected, just as observed in Figs. 5—7. Second, since the theoretical peak frequency depends on emission angle and phonon polarization, it is not surprising that the signal increase occurred at different N_s values under the different experimental conditions. Third, the dependence of the signal size on the carrier drift direction (phonon-drag effect) which was found experimentally (Fig. 7) is also expected theoretically (Fig. 9). Fourth, the broadening of the increase in Fig. 7 with larger electrical power levels can be ascribed to a larger thermal smearing of the $2k_F$ cutoff.

To compare experiment and theory quantitatively we calculated the phonon spectra using the parameters of our sample. The spectra were then integrated over the respective detection bands, taking the precise shape of the isotope scattering into account. The resulting phonon intensities as a function of N_s are plotted in Figs. 4—7 as dashed lines. A scale factor was used as the only adjustable parameter.

The comparison of theory and experiment shows that the steep signal increase is very well reproduced under all conditions. The size of the phonon-drag effect in Fig. 7 is also very well described by theory.

An analysis of the pertinent parameters revealed that the k_F value needed to be correct within less than 5% to reproduce the signal increase at the measured N_s value. This verifies relation (2). The electron temperature, however, did not affect the shape of the increase as long as it was below about 25 K.

Other features in the experimental data, such as the hump ($N_s = 5 \times 10^{12}$ cm^{-2}) and the signal decrease ($N_s = 6 \times 10^{12}$ cm^{-2}), could not be explained from our theory. Interestingly, the signal measured with the broadband Al detector turned out to deviate from theory in the same range of N_s values. We cannot explain these anomalies at present. We suspect, however, that they are caused by the population of higher subbands which lie close to E_F at large electron densities.[1,22] The influence of the higher subbands could possibly be tested by applying uniaxial stress. Such experiments are presently underway.

We did not attempt to fit the results at higher E_{SD} fields in Fig. 7. Calculating the temperature T_{el} within our model would have involved phonon modes close to the zone edge of Si. In this regime the simple model is bound to fail.

During the entire work, we always took data also with the holes. No interesting structures were ever observed. This is probably a consequence of the more complicated band structure which allows more possibilities for a hole transition, particularly those involving phonons with small q values.

VI. CONCLUSIONS

It has been demonstrated, both experimentally and theoretically, that the lower dimensionality of the electrons, as well as the Fermi statistics, influence the emitted phonon spectra profoundly. The reduced dimensionality of the 2D EG leads to the reduction of the momentum conservation to the components in the plane. This effect led to the angle dependence of the phonon spectra.

The Fermi statistics caused the $2k_F$ cutoff which was very well reproduced in the experiments. The cutoff also tested the theoretical k_F values. This k_F-testing possibility of phonon spectroscopy may be exploited further in other 2D systems.

The phonon spectra, however, behaved as expected only as long as N_s was less than 5×10^{12} cm^{-2}. It is possible that the influence of the higher subbands must be considered in the theory at larger N_s values. We will study this further and hope to learn more about transitions between different subbands.

Another point which deserves more investigation is the phonon-drag effect. The observation of dramatic phenomena such as Cerenkov-like phonon radiation may be possible in high-mobility samples prepared as GaAs heterostructures.

ACKNOWLEDGMENTS

It is a pleasure to thank Professor H. Kinder for his constant interest in this work and for the many valuable suggestions he has made. The advice of the members of Professor F. Koch's institute, especially of A. Zrenner, was very helpful for our understanding of MOS devices. We are very thankful to Dr. J. Kemmer for his readiness to grow the oxides. The stimulus of this work came from an earlier cooperation with Professor J. Kotthaus.

[1]For a review, see T. Ando, A. B. Fowler, and F. Stern, Rev. Mod. Phys. **54**, 437 (1982).

[2]J. C. Hensel, R. C. Dynes, and D. C. Tsui, J. Phys. (Paris) Colloq. **42**, C6-308 (1981); J. C. Hensel, B. I. Halperin, and R. C. Dynes, Phys. Rev. Lett. **51**, 2302 (1983).

[3]M. A. Chin, V. Narayanamurti, H. L. Störmer, and J. C. M. Hwang, in *Phonon Scattering in Condensed Matter,* Vol. 51 of *Springer Series in Solid-State Sciences,* edited by W. Eisenmenger, K. Lassman, and S. Döttinger (Springer-Verlag, Berlin, 1984), p. 328.

[4]T. Neugebauer and G. Landwehr, Phys. Rev. B **21**, 702 (1980).

[5]R. A. Höpfel, E. Vass, and E. Gornik, in *Phonon Scattering in Condensed Matter,* Vol. 51 of *Springer Series in Solid-State Sciences* edited by W. Eisenmenger, K. Lassmann, and S. Döttinger (Springer-Verlag, Berlin, 1984), p. 331.

[6]Wacker Chemitronic, Burghausen, Federal Republic of Germany.

[7]The oxides were grown either by Wacker Chemitronic or by Dr. J. Kemmer, Diodenlabor, Physik-Department, Technische Universität München.

[8]We had occasionally used electron inversion layers in *p*-doped Si. The phonon results showed no difference from those of accumulation layers.

[9]V. Dolgopolov, C. Mazuré, A. Zrenner, and F. Koch, J. Appl. Phys. **55**, 4280 (1984).

[10]P. Herth and O. Weis, Acustica **21**, 162 (1969); P. Berberich (private communication).

[11]For a review on heat pulses, see, e.g., V. Naraynamurti, Science **213**, 717 (1981).

[12]W. Eisenmenger, in *Physical Acoustics,* edited by W. P. Mason and R. N. Thurston (Academic, New York, 1976), Vol. 12, p. 80.

[13]H. J. Maris, J. Acoust. Soc. Am. **50**, 812 (1971); G. A. Northrop and J. P. Wolfe, Phys. Rev. B **22**, 6196 (1980).

[14]P. G. Klemens in *Solid State Physics,* edited by F. Seitz and D. Turnbull (Academic, New York, 1958), Vol. 7, p. 1.

[15]W. Dietsche, G. A. Northrup, and J. P. Wolfe, Phys. Rev. Lett. **47**, 660 (1981).

[16]S. Tamura, Phys. Rev. B **25**, 1415 (1982).

[17]G. Simmons and H. Wang, *Single Crystal Elastic Constants and Calculated Aggregate Properties* (MIT Press, Cambridge, Mass., 1971).

[18]M. Rothenfusser, W. Dietsche, and H. Kinder, Phys. Rev. B **27**, 5196 (1983).

[19]E. Vass, Solid State Commun. **55**, 847 (1985).

[20]C. Herring and E. Vogt, Phys. Rev. **101**, 944 (1956).

[21]Its explicit form is taken from Ref. 1 as formula (2.52).

[22]U. Kunze, Phys. Rev. B **32**, 5328 (1985).